ACTA ONCOLOGICA
2022, VOL. 61, NO. 2, 247–254
https://doi.org/10.1080/0284186X.2021.1967445

Taylor & Francis
Taylor & Francis Group

ORIGINAL ARTICLE

Check for updates

Atlas-based auto-segmentation for delineating the heart and cardiac substructures in breast cancer radiation therapy

Marie Louise H. Milo[a], Tine B. Nyeng[b], Ebbe L. Lorenzen[c], Lone Hoffmann[b,d], Ditte S. Møller[b,d] and Birgitte V. Offersen[a,e,f]

[a]Department of Experimental Clinical Oncology, Aarhus University Hospital, Aarhus, Denmark; [b]Department of Medical Physics, Aarhus University Hospital, Aarhus, Denmark; [c]Laboratory of Radiation Physics, Odense University Hospital, Odense, Denmark; [d]Department of Clinical Medicine, Faculty of Health Sciences, Aarhus University, Denmark; [e]Danish Centre for Particle Therapy, Aarhus University Hospital, Aarhus, Denmark; [f]Department of Oncology, Aarhus University Hospital, Aarhus, Denmark

ABSTRACT

Background: This study aimed to develop and validate an automatic multi-atlas segmentation method for delineating the heart and substructures in breast cancer radiation therapy (RT).

Material and methods: The atlas database consisted of non-contrast-enhanced planning CT scans from 42 breast cancer patients, each with one manual delineation of the heart and 22 cardiac substructures. Half of the patients were scanned during free-breathing, the rest were scanned during a deep inspiration breath-hold. The auto-segmentation was developed in the MIM software system and validated geometrically and dosimetrically in two steps: The first validation in a small dataset to ensure consistency of the atlas. This was succeeded by a final test where multiple manual delineations in CT scans of 12 breast cancer patients were compared to the auto-segmentation. For geometric evaluation, the dice similarity coefficient (DSC) and the mean surface distance (MSD) were used. For dosimetric evaluation, the RT doses to each substructure in the manual and the automatic delineations were compared.

Results: In the first validation, a high geometric and dosimetric performance between the automatic and manual delineations was observed for all substructures. The final test confirmed a high agreement between the automatic and manual delineations for the heart (DSC = 0.94) and the cardiac chambers (DSC: 0.75–0.86). The difference in MSD between the automatic and manual delineations was low (<4 mm) in all structures. Finally, a high correlation between mean RT doses for the automatic and the manual delineations was observed for the heart and substructures.

Conclusions: An automatic segmentation tool for delineation of the heart and substructures in breast cancer RT was developed and validated with a high correlation between the automatic and manual delineations. The atlas is pivotal for large-scale evaluations of radiation-associated heart disease.

ARTICLE HISTORY
Received 25 June 2021
Accepted 5 August 2021

KEYWORDS
Atlas based auto-segmentation; cardiac substructures; breast cancer; radiation therapy

Introduction

Radiation therapy (RT) is widely used in the adjuvant treatment of early breast cancer to reduce the risk of recurrence and breast cancer death [1,2]. In recent years, the awareness of radiation-associated cardiac toxicity, particularly coronary artery disease, has increased [3,4]. A linear dose-response relationship between mean heart dose and the risk of coronary artery disease has been demonstrated [4–6]. Optimizations of RT regimens and implementation of deep inspiration breath-hold (DIBH) during treatment have resulted in a reduction in mean heart dose [7–9]. However, when using the most prevalent technique of tangential fields, the dose distribution in the heart is heterogeneous and small parts of the heart may receive a high dose where the dose deposition is highly dependent on patient anatomy, the target, and laterality of irradiation [10–12]. Recently, studies have shown conflicting results regarding mean heart dose as a predictor for cardiac toxicity [10,13]. Thus, more knowledge regarding clinical effects from RT doses to the heart and substructures during modern CT-based RT is important to support further epidemiological studies and clinical trials investigating radiation-associated cardiac toxicity. A cardiac contouring atlas for delineation of the heart and substructures is available, however, manual delineation is time-consuming, not a routine task and subject to uncertainty [14,15]. Among experts, the mean surface distance (MSD) ranged between 1 and 3 mm for the heart and the cardiac chambers and 2–10 mm for the coronary artery segments [15].

Auto-segmentation has the capacity to increase the efficacy and reproducibility of cardiac contouring. In recent years, several auto-segmentation algorithms have been developed [16–25]. Some algorithms focus on delineation of the left anterior descending coronary artery (LADCA) from anatomical landmarks or by adding a planning organ at risk

CONTACT Marie Louise H. Milo milo@oncology.au.dk Department of Experimental Clinical Oncology, Aarhus University Hospital, Palle Juul-Jensens Boulevard 99, Aarhus N, 8200, Denmark

Supplemental data for this article can be accessed here.

© 2021 Acta Oncologica Foundation

volume [16–18]. Other algorithms include several structures as the cardiac chambers, the coronary arteries, the substructures of the left ventricle wall, and/or the heart valves [19–25]. All auto-segmentation models are evaluated geometrically and some also dosimetrically [19,23,24]. The most exposed substructures after left-sided tangential breast cancer RT are the anterior/apical part of the left ventricle wall and the middle/distal part of LADCA and after right-sided RT, the proximal part of the right coronary artery (RCA) is most exposed [11]. One study reports a geometric validation of auto-segmentation of the left ventricle wall and the coronary arteries segmented in ten substructures [21]. However, the most important feature in auto-segmentation is the accuracy of the reported RT dose. Thus, the aim of this study was to develop an automatic multi-atlas-segmentation method for delineating the heart and cardiac substructures including the cardiac chambers, left ventricle wall, segmentation of the coronary arteries, and the large vessels in non-contrast-enhanced planning CT scans of breast cancer patients. Furthermore, the aim was to evaluate the auto-segmentation, both geometrically and dosimetrically, compared to multiple manual delineations.

Material and methods

Selection of CT scans for generating an atlas database

The atlas database consisted of planning CT scans from 42 early breast cancer patients irradiated during 2019 and 2020 at two centers. The CT scans were selected randomly, irrespective of tumor laterality and type of surgery. Seventeen patients were treated at Odense University hospital (OUH) whilst 25 were treated at Aarhus University Hospital (AUH). All CT scans were non-contrast-enhanced and acquired with 3 mm slice separation in supine position with both arms (OUH) or the ipsilateral arm (AUH) elevated. DIBH was used when indicated (RT of left-sided breast only or loco-regional RT regardless of laterality, $n = 21$). Patients with thorax deformities such as pectus excavatum and scoliosis were also included in the atlas database.

Manual delineation for atlas generation

The heart and 22 substructures, including 18 cardiac substructures (the four cardiac chambers, four segments of the left ventricle wall, and ten coronary artery segments) and 4 large vessels (ascending aorta, pulmonary trunk, superior and inferior vena cava) were manually delineated in the 42 planning CT scans by one of 14 clinical oncologists or two radiation physicists. All represented one of the four Danish Multidisciplinary Cancer Groups (the Danish Breast Cancer Group, the Danish Lung Cancer Group, the Danish Lymphoma Group and the Danish Esophageal, Gastroesophageal and Ventricle Cancer Group) and they all treated cancer patients where incidental RT to the heart may be of concern. The delineations of the heart and substructures were performed according to Danish national guidelines and were subsequently audited by one oncologist (MLHM) to ensure accuracy and consistency according to the guidelines [15].

Auto-segmentation methods

The atlas and post-processing workflows for auto-segmentation were developed in MIM version 7.0.4 (MIM Software, Cleveland, OH, USA) (Figure 1). The CT scan of a patient with typical thoracic anatomy was selected as the main template for initial rigid registration. All other CT scans were aligned to this template using the left ventricle as the region of

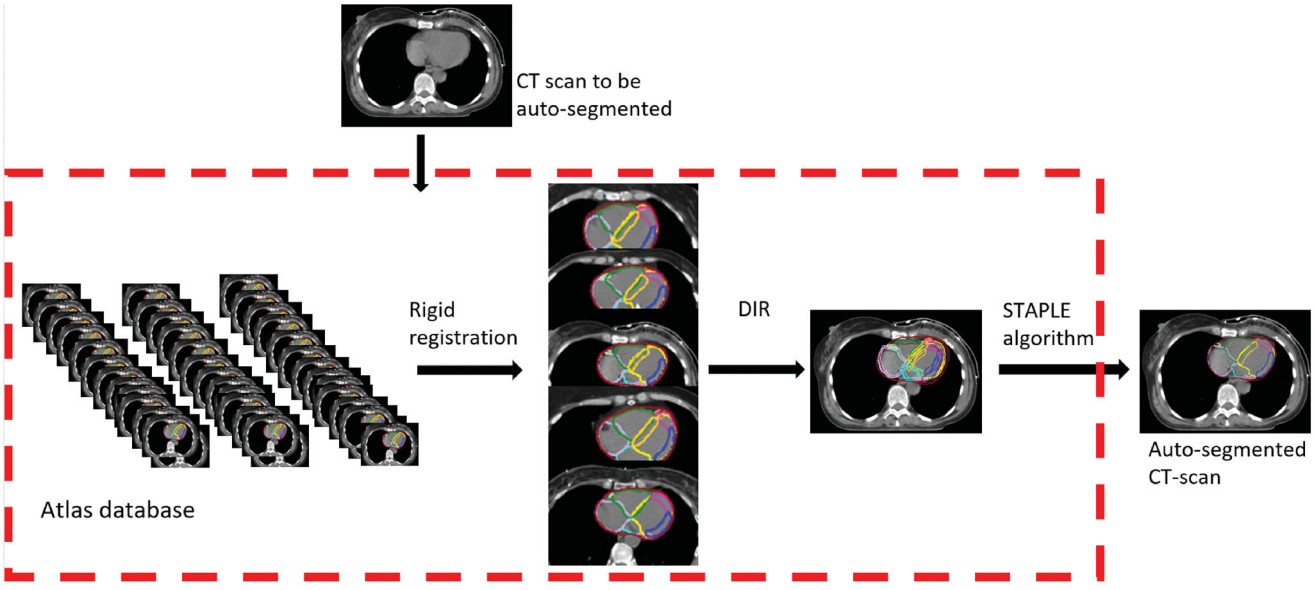

Figure 1. The process of auto-segmentation consists of three steps. (1) A rigid registration between the CT scans in the atlas database and the CT scan to be auto-segmented aiming to obtain the five CT scans with the highest anatomical match. However, for auto-segmentation of the left ventricle wall, only three subjects were used as this resulted in a higher delineation consistency than when using five subjects. (2) The selected CT scans were submitted to the deformable image registration (DIR) algorithm where the suggestion for each structure for the selected patients were transferred to the new CT scan. (3) Finally, the simultaneous truth and performance level estimation (STAPLE) algorithm was used to collapse the multiple delineations into one delineation.

interest. To ensure an optimal segmentation of the coronary arteries, automatically generated isotropic margins of 5 mm were saved to the atlas instead of the anatomical structures. The atlas was run using the multi-modality free-form deformable image registration (DIR) algorithm VoxAlign® in MIM, the precision of which has been documented by Piper et al. [26]. Multiple atlas subjects (five for the heart, chambers, coronary artery segments and large vessels, three for the left ventricle wall) were deformably registered for each auto-segmentation. The multiple suggestions for each anatomical structure were combined and finalized using the Simultaneous Truth and Performance Level Estimation (STAPLE) expectation-maximization algorithm [27]. Following auto-segmentation, several automatic post-processing steps were carried out: all contours were smoothed by expanding and then contracting by 5–10 mm. The ten coronary artery segment margins were additionally contracted by 4 mm to represent the anatomical structures. Individual cranial or caudal slices of the whole heart contour were removed automatically if they were smaller than 9 mm^2 (cranial) or 4 mm^2 (caudal) and the structures were then smoothed and possible holes filled in. Finally, all volumes except the inferior vena cava were cropped so as not to protrude outside the whole heart structure.

Validation of the atlas-based auto-segmentation

The atlas was built by iteratively adding CT scans and structure delineations while testing the outcome. Two consecutive tests of the atlas were performed (Supplementary Figure 1): The first step of validation in six breast cancer patients treated at AUH (three patients were scanned under free-breathing and three during DIBH) with the heart and substructures delineated both manually (MLHM) and automatically. The aim of the first validation was to investigate if further adjustments in the auto-segmentation workflow were needed to achieve acceptable results in line with the inter-observer variability previously observed [15]. A second step for final testing of the auto-segmentation was performed in a dataset of 12 CT scans where four patients were scanned under free-breathing and eight during DIBH. Each CT scan had five independent manual delineations of the heart and substructures contoured by 14 clinical oncologists and two radiation physicists during a two-day workshop aiming to obtain and validate cardiac contouring guidelines. Detailed information regarding the dataset was presented previously [15].

All the patients were retrospectively treated with tangential fields in addition to an anterior and/or posterior field if the regional lymph nodes were included in the target. The dose prescription was 40 Gy in 15 fractions for breast only and 50 Gy in 25 fractions for loco-regional irradiation. The heart and LADCA were routinely delineated as organs at risk and according to the Danish Breast Cancer Group guidelines, the dose constraints were: V20 Gy $<$ 10%, V40 Gy $<$ 5% and maximum dose to LADCA $<$ 17 Gy.

Statistical evaluation

Before analyses were performed, the automatic delineations were visually assessed by one oncologist (MLHM). Two metrics were used for geometric evaluation: the Sørensen-Dice similarity coefficient (DSC) and the MSD. The DSC describes the overlap between two delineations and the value ranges between zero (no overlap) and one (perfect overlap). The MSD describes the mean of the shortest distance from any surface point of one delineation to the surface of the other delineation. For the final test, the automatic delineation for each patient and each substructure was compared to each of the five corresponding manual delineations. The manual delineations were each compared to the remaining four manual delineations. The DSC and the MSD were reported as the median value and the *p*-values, testing for no difference in metrics between the automatic and manual delineations were calculated by using Wilcoxon signed-rank test.

In the first validation, the dosimetric evaluations were performed by comparing the RT doses as delivered to the automatic and manual delineations. In the final test, the mean RT doses to the heart and each substructure were compared between the dose delivered to the automatic delineation and the RT dose determined in each of the five manual delineations (Supplementary Figure 2). The correlation between RT doses derived from the automatic and manual contours was tested according to the x = y line (line of identity) and assessed with the Root Mean Squared Error (RMSE). Lower RMSE indicates a better fit. The second step of final testing was done by an external expert (ELL) who was not involved in the development of the atlas and the first validation. The study was designed in harmony with the agree-reporting checklist 2016 [28].

Results

In the first step of validation, some inconsistencies between the substructures were observed in the auto-segmentation. At the cranial and caudal boundaries, some overlap between substructures was seen. For the coronary arteries, the delineation could be missing in one CT slice in the transition between two substructures. The overlap between the auto-segmentation and the manual delineation was highest for the heart (mean DSC = 0.94) and the four cardiac chambers with mean DSC ranging between 0.81 and 0.89 (Supplementary Figure 3). No systematic difference was observed for patients scanned during free breathing (patient 1–3) versus DIBH (patient 4–6). A linear correlation between RT doses in the automatic and the manual delineations was observed for the heart and substructures, with an RMSE $<$ 0.5 Gy (Supplementary Figure 4).

In the second step of final testing, the visual performance of the atlas was acceptable, however, the automatic segmentation failed for the posterior descending artery in five of the 12 patients and for the distal part of the RCA in one of the 12 patients. For all the remaining structures, the automatic delineations performed well. The DSC between the auto-segmentation and the manual delineations was 0.94 for the

heart and ranged between 0.75 and 0.86 for the cardiac chambers. In comparison, the DSC between the manual delineations was 0.94 for the heart and ranged between 0.80 and 0.88 for the cardiac chambers. In general, the DSC decreased with smaller structures (Figure 2). The MSD between the automatic and manual delineations was slightly higher than the MSD between the manual delineations (Figure 3). For the heart, the difference in MSD between the automatic and manual delineations was 0.4 mm and for the chambers the difference ranged between 0.4 mm for the left ventricle and 0.9 mm for the left atrium and the right ventricle. In general, the difference in MSD between the

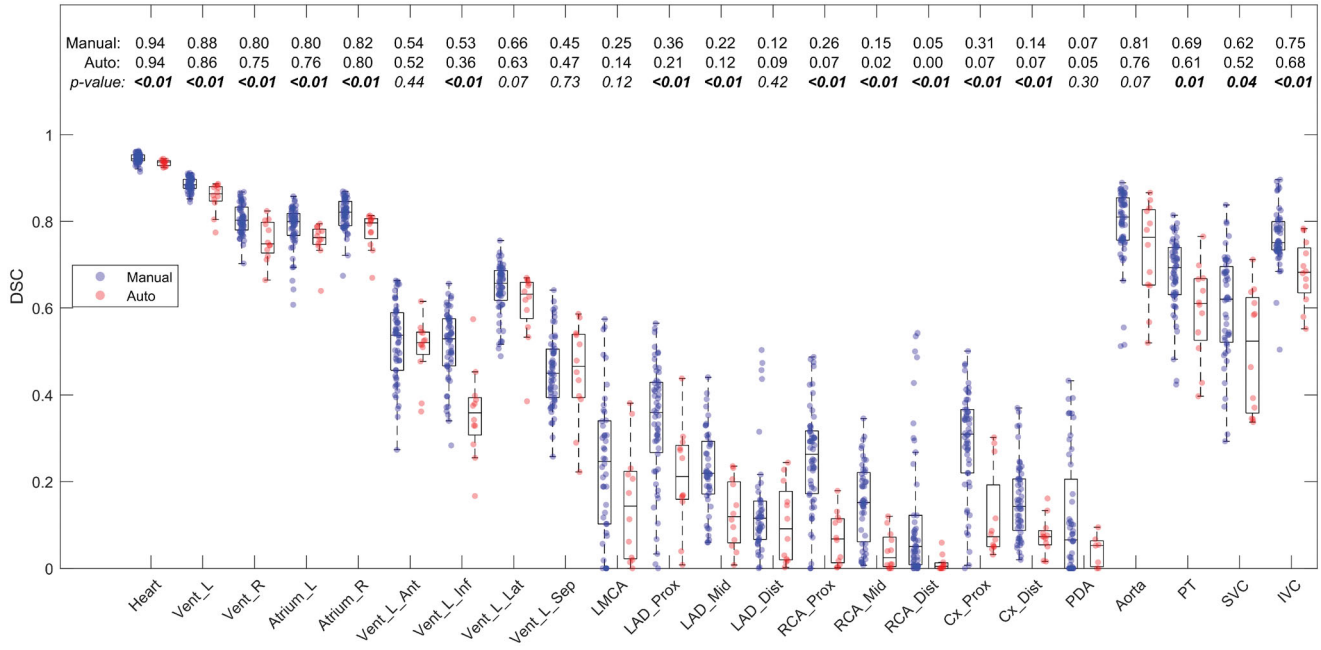

Figure 2. Boxplot of the DSC between the 60 manual delineations (blue dots) performed by 16 observers in CT scans of 12 breast cancer patients and between the automatic and manual delineations (red dots) for the heart and substructures in the final test. Median values for manual and automatic delineations are given at the top, with corresponding *p*-values for the difference. Abbreviations: Heart: Whole heart; Vent: Ventricle; L: Left; R: Right; Ant: Anterior; Lat: Lateral; Inf: Inferior; Sep: Septal; LMCA: Left Main Coronary Artery; LAD: Left Anterior Descending coronary artery; Cx: Circumflex coronary artery; RCA: Right Coronary Artery; PDA: Posterior Descending Artery; Prox: Proximal; Mid: Middle; Dist: Distal; PT: Pulmonary Trunk; SVC: Superior Vena Cava; IVC: Inferior Vena Cava.

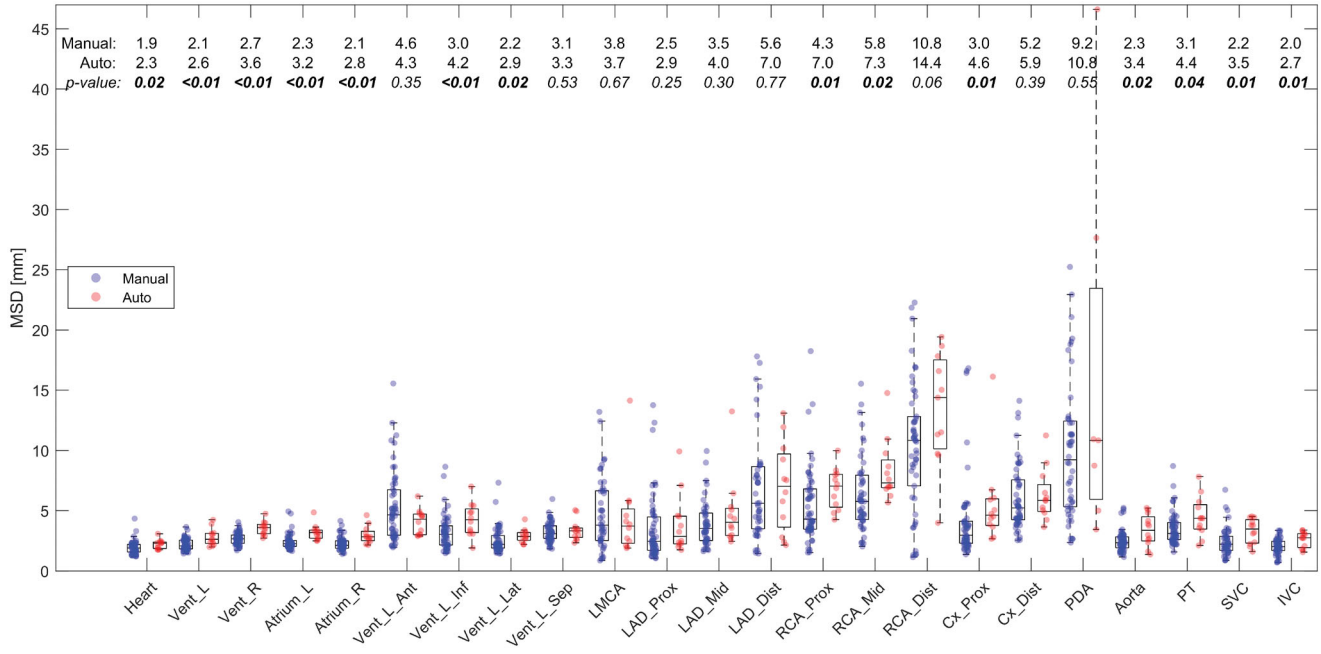

Figure 3. Boxplot of the MSD between the 60 manual delineations, (blue dots) performed by 16 observers in CT scans of 12 breast cancer patients and between the automatic and manual delineations (red dots) for the heart and substructures in the final test. Median values for manual and automatic delineations are given at the top, with corresponding *p*-values for the difference. Abbreviations: Heart: Whole heart; Vent: Ventricle; L: Left; R: Right; Ant: Anterior; Lat: Lateral; Inf: Inferior; Sep: Septal; LMCA: Left Main Coronary Artery; LAD: Left Anterior Descending coronary artery; Cx: Circumflex coronary artery; RCA: Right Coronary Artery; PDA: Posterior Descending Artery; Prox: Proximal; Mid: Middle; Dist: Distal; PT: Pulmonary Trunk; SVC: Superior Vena Cava; IVC: Inferior Vena Cava.

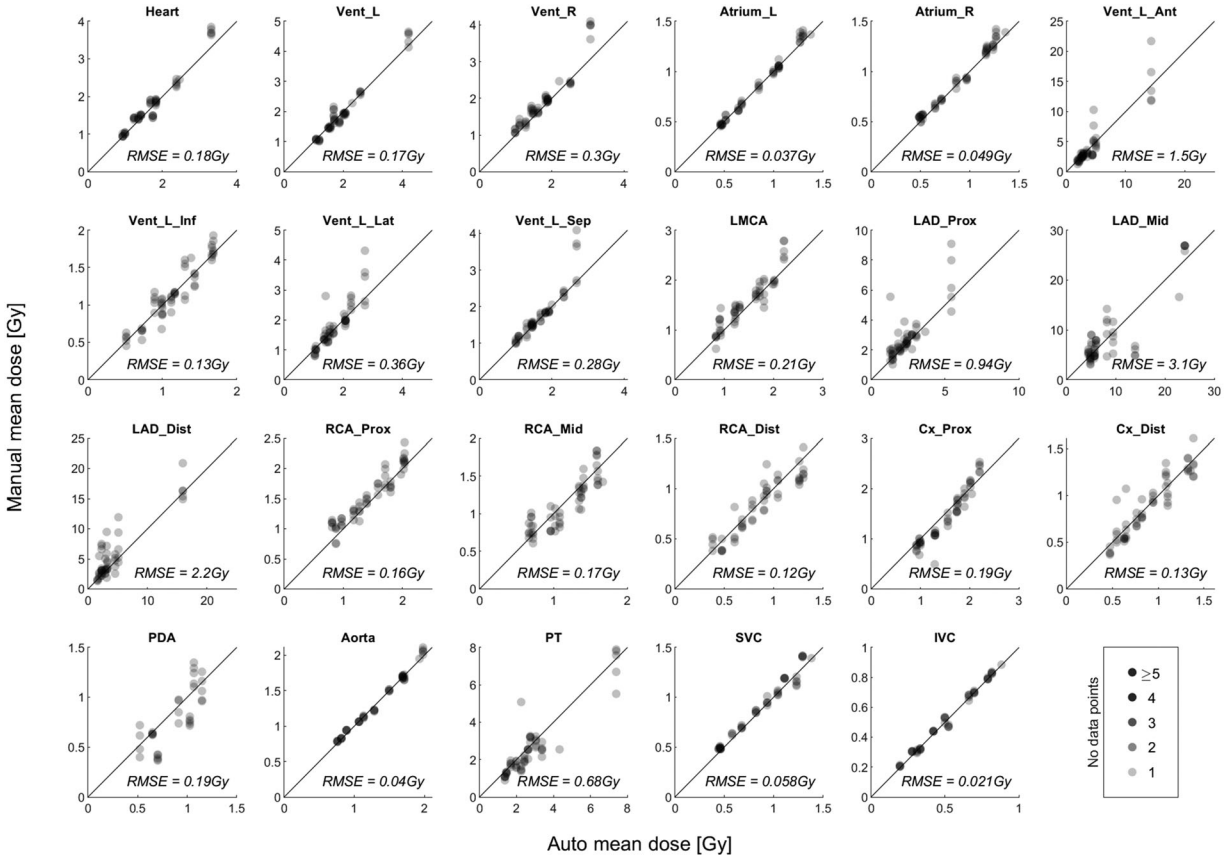

Figure 4. The correlation between RT doses in the automatic delineations (x-axis) and the five manual delineations (y-axis) for the heart and substructures in the final test. The line is x = y (line of identity) where the light gray dots located vertically indicates the variation in the manual delineations. Abbreviations: Heart: Whole heart; Vent: Ventricle; L: Left; R: Right; Ant: Anterior; Lat: Lateral; Inf: Inferior; Sep: Septal; LMCA: Left Main Coronary Artery; LAD: Left Anterior Descending coronary artery; Cx: Circumflex coronary artery; RCA: Right Coronary Artery; PDA: Posterior Descending Artery; Prox: Proximal; Mid: Middle; Dist: Distal; PT: Pulmonary Trunk; SVC: Superior Vena Cava; IVC: Inferior Vena Cava.

automatic and manual delineations was low with a median difference in MSD <2 mm for all substructures except the proximal and distal part of the RCA (<4 mm).

The best correlation between mean RT doses for the automatic and the mean RT doses for the manual delineations was observed for the heart (RMSE = 0.18 Gy) and the four cardiac chambers (RMSE ranged between 0.037 Gy and 0.30 Gy). For the vast majority of the structures, the correlation was high, with RMSE <1 Gy, except for the anterior segment of the left ventricle and the middle and distal part of the LADCA (Figure 4).

Discussion

In this study, an automatic CT-based atlas for delineation of the heart and 22 substructures was developed and validated. The validation consisted of two steps, both including a geometric and dosimetric comparison between automatic and manual delineations. The delineation uncertainty between the automatic and manual delineations was in the same range as the uncertainty observed between the manual delineations performed by experts. The dosimetric comparison showed high agreement between doses obtained for the automatic and the manual delineations including the small structures, suggesting that the auto-segmentation method could be a feasible tool in studies aiming to evaluate doses to the heart and substructures after RT for early breast cancer. The highest difference in RT doses between the automatic and manual delineations was observed for the middle and distal part of the LADCA and the anterior segment of the left ventricle. For left-sided tangential field-based RT, these three substructures are located near the RT field, thus, even small changes in the position may cause substantial differences in the RT dose.

In both validation sets used in this study, some patients were scanned during free breathing and others during DIBH which shifts the heart in a caudal and dorsal direction away from the treatment field, and this may change the anatomy of the heart [8]. However, the CT scan to be auto-segmented was registered to the five best-fitting CT scans from the database, which included patients treated with either free breathing or DIBH, by matching on the left ventricle to minimize the patient-to-patient variation. This increases the applicability of auto-segmentation in large cohorts where information on DIBH may be missing.

The variation between the automatic and manual delineations of the heart and substructures observed in our study is in agreement with the variation reported in other studies (Table 1) [19–25]. In these studies, as in our, an increasing variation between the automatic and manual delineations was observed with smaller structures [20–23]. This is expected, as the main differences occur at the boundary,

Table 1. Comparison of the method, sample size, and structures for auto-segmentation using atlas-based approach published in the recent years.

Study	Method	Sample size	Chambers (DSC)	Left ventricle wall (DSC)	Coronary arteries (DSC)	Large vessels (DSC)	Evaluating
Maffei et al. [21][a,b]	Hierarchical clustering Non-contrast CT	36 (atlas + cross-validation)	Heart (0.94) Chambers (0.76–0.87)	Five substructures[c] (0.50–0.61)	LMCA (0.19) LADCA, 3 seg (0.04–0.19) RCA, 4 seg (0.06–0.16) Cx, 2 seg (0.17–0.27)	Asc aorta (0.77) PT (0.77) SVC (0.68) IVC (0.59)	Geometric (DSC, HD)
Loap et al. [22]	Multi-atlas Non-contrast CT	20 (atlas) 20 (validation)	Heart (0.95) Chambers (0.76–0.87)	Five substructures[c] (0.50–0.61)	–	–	Geometric (DSC, volumes)
Morris et al. [23] [a,d,e,f]	Multi-atlas Registration with MRI/ Non-contrast CT	20 (atlas) 11 (validation)	Heart (0.95) Chambers (0.83–0.91)	–	LMCA (0.12) LADCA (0.27) RCA (0.22)	Asc aorta (0.84) PT (0.84) SVC (0.80) IVC (0.70)	Geometric (DSC, MSD, centroid displacement) Dosimetric
Kaderka et al. [19] [a,d]	Multi-atlas Non-contrast CT	27 (atlas) 27 (validation)	Heart (0.93) Chambers (0.76–0.85)	–	LADCA (0.09)	–	Geometric (DSC, HD) Dosimetric
Finnegan et al. [13,20]	Multi-atlas Leave one out Non-contrast CT	20 (atlas + cross-validation)	Heart (0.94) Chambers (0.82–0.86)	–	LMCA(0.12) LADCA (0.05) RCA (0.04) Cx (0.06)	Asc aorta (0.80) Dec aorta (0.85) PT (0.67) SVC (0.55)	Geometric [20] (DSC, MSD) Dosimetric [13]
Jung et al. [24]	Multi-atlas Leave one out Non-contrast CT	30 (atlas + cross-validation)	Heart (0.97) Chambers (0.65–0.80)	–	LMCA (NA) LADCA (NA) RCA (NA) Cx (NA)	–	Geometric (DSC, MSD) Dosimetric
Zhou et al. [25][a]	Multiatlas segmentation Contrast CT	12 (atlas) 19 (validation)	Heart (0.95) Chambers (0.76–0.81)	–	LMCA (0.24) LADCA (0.15) RCA (0.18) Cx (0.32)	Asc aorta (0.78) PT (0.82) SVC (0.66) IVC (0.64)	Geometric (DSC, MSD)
This work[a,d]	Multi-atlas Non-contrast CT	42 (atlas) 60 (validation) (12 CT-scans/5 delineations)	Heart (0.94) Chambers (0.75–0.86)	Four substructures[g] (0.36–0.63)	LMCA (0.14) LADCA, 3 seg (0.09–0.21) RCA, 4 seg (0.00–0.07) Cx, 2 seg (0.00–0.07)	Asc aorta (0.76) PT (0.61) SVC (0.55) IVC (0.68)	Geometric (DSC, MSD) Dosimetric

[a]Simultaneous Truth and Performance Level Estimation (STAPLE algorithm was used).
[b]DSC values are reported for STAPLE algorithm.
[c]Delineated according to Duane et al.
[d]MIM software was used for auto segmentation.
[e]The CT scans were rigid registered with magnetic resonance imaging to improve the visibility of cardiac structures.
[f]DSC values are reported for STAPLE algorithm (10 patients).
[g]Delineated according to Milo et al.
Abbreviations: DSC: Dice similarity coefficient, LMCA: Left main coronary artery, LADCA: Left anterior descending coronary artery, seg: Segments, RCA: Right coronary artery, Cx: circumflex coronary artery, Asc: Ascending, PT: Pulmonary trunk, SVC: superior vena cava, IVC: Inferior vena cave, HD: Hausdorff Distance, MSD: Mean Surface Distance.

however, several other explanations may also be in play: First, non-contrast-enhanced CT scans are routinely used in RT planning for breast cancer making it difficult to identify the coronary arteries both in manual and automatic delineations. Some studies used contrast-enhanced CT scans resulting in better geometric results for the heart but for the coronary arteries, the DSC was still <0.4, thus the variation was in the same magnitude as in our study [25]. Second, the cardiac and respiratory motion will cause displacement of the heart and coronary arteries. A planning organ at risk volume has been suggested to overcome this motion artifact [17]. For optimizing of the segmentation, we used a 5 mm isotopic margin in the delineation of the coronary arteries, however, it was followed by a contraction of 4 mm to represent the anatomical structures. Third, an atlas-based auto-segmentation model is not able to adjust for normal variations of the coronary artery anatomy. Most commonly, the posterior descending artery is generated from the RCA (70–80% of the population) but can also derivate from an anastomosis between the RCA and the circumflex artery (10–20% of the population) or the circumflex artery alone (5–10% of the population) [29]. This atlas is designed to delineate the posterior descending artery from the RCA. In our study, the coronary arteries were divided into 10 segments in accordance with the Danish guidelines [15]. Segmentation of the coronary arteries, especially the separation between the middle and distal parts of the RCA and LADCA, is difficult due to weak anatomical landmarks. Several studies report auto-segmentation of the three main coronary arteries, [20,21,23–25] however, the dose difference in the segments of one coronary artery may differ substantially. To our knowledge, only one auto-segmentation algorithm managed to delineate sub-segments of the coronary arteries which may be important in investigating cardiac toxicity [21]. That study reported geometric validation by DSC in accordance with our results, however, a dosimetric validation was not performed. In a study by Kadeka et al., a dosimetric evaluation of the entire LADCA showed a linear correlation between the automatic and manual delineations, as observed for the segments in our study [19].

The atlas database established for this study, contained female breast cancer patients only and moreover, the auto-segmentation was validated in breast cancer patients. However, for other cancer subtypes as lymphoma, lung and esophageal cancer, incidental RT dose to the heart may also be of concern. The performance of the atlas may decrease substantially in CT scans of patients with these cancer types and in males due to differences in RT regimens and anatomy. The reported variation in RT dose is highly dependent on the dose distribution, thus further studies are needed before extrapolating to other cancer sites.

There are several strengths in this study. The iterative evaluation of the subjective performance of the atlas during the phase of atlas-building ensured a sufficient number of CT scans in the database to secure a high quality, with a total of 42 patients. It has been shown that a high number of CT scans in the database improves segmentation results [21]. Also, the auto-segmentation was tested against multiple manual delineations performed by experts and considered as the "gold standard". Furthermore, the RT planning CT scans used in the atlas database represented a random variation of anatomy among early breast cancer patients and differences in the positioning (one or two arms elevated) which may influence the position of the heart. Additionally, the CT scans were without IV-contrast, non-ECG gated and, for half of the patients, obtained under free breathing. Thus, the database constitutes a heterogeneous and representative group of breast cancer patients. Finally, the results of the second step of final testing were analyzed by an external expert (ELL) not involved in the development of the atlas. A limitation in this study was the failure to auto-segment some of the smaller structures (the posterior descending artery in five patients and the distal part of RCA in one patient). These structures are present in only a few CT slices which may give rise to failure in the segmentation. Generally, the atlas was successful in segmenting the small structures when replacing them with 5 mm isotropic expansions. Furthermore, the manual delineation of these structures also suffered from high inter-observer variation [15].

In conclusion, we developed a method for auto-segmentation of the cardiac chambers, substructures of the left ventricle, the coronary arteries, and the large vessels in breast cancer RT. The differences in median MSD between the automatic and manual delineations were <2 mm, except for the proximal and distal parts of RCA. The correlation between RT doses to the automatic and manual delineations was high with an RMSE <1 Gy for all cardiac substructures, except LADCA. The atlas will be used for large-scale evaluations of radiation-associated heart disease (work in progress).

Acknowledgments

The authors thank the Danish Comprehensive Cancer Center Onco-Cardiology Group and Novo Nordisk Fonden.

MIM Software Inc. Cleveland, OH is acknowledged for providing a license for research use of the MIM software.

Disclosure statement

No potential conflict of interest was reported by the author(s).

Funding

MLHM, ELL, LH, DSM, and BVO are supported by DCCC Radiotherapy – The Danish National Research Center for Radiotherapy (grant no R191-A11526). Furthermore, MLHM is supported by Danish Cancer Society and Aarhus University. DSM is supported by Danish Cancer Society (grant no. R209-A13036). BVO is supported by Danish Cancer Society and Novo Nordisk Fonden.

ORCID

Lone Hoffmann http://orcid.org/0000-0002-3575-0421

References

[1] Darby S, McGale P, Correa C, et al. Effect of radiotherapy after breast-conserving surgery on 10-year recurrence and 15-year breast cancer death: meta-analysis of individual patient data for 10 801 women in 17 randomised trials. Lancet. 2011;378: 1707–1716.

[2] McGale P, Taylor C, Correa C, et al. Effect of radiotherapy after mastectomy and axillary surgery on 10-year recurrence and 20-year breast cancer mortality: meta-analysis of individual patient data for 8135 women in 22 randomised trials. Lancet. 2014;383: 2127–2135.

[3] McGale P, Darby SC, Hall P, et al. Incidence of heart disease in 35,000 women treated with radiotherapy for breast cancer in Denmark and Sweden. Radiother Oncol. 2011;100(2):167–175.

[4] Darby SC, Ewertz M, McGale P, et al. Risk of ischemic heart disease in women after radiotherapy for breast cancer. N Engl J Med. 2013;368(11):987–998.

[5] Laugaard Lorenzen E, Christian Rehammar J, Jensen MB, et al. Radiation-induced risk of ischemic heart disease following breast cancer radiotherapy in Denmark, 1977–2005. Radiother Oncol. 2020;152:103–110.

[6] Van Den Bogaard VAB, Ta BDP, Van Der Schaaf A, et al. Validation and modification of a prediction model for acute cardiac events in patients with breast cancer treated with radiotherapy based on three-dimensional dose distributions to cardiac substructures. J Clin Oncol. 2017;35(11):1171–1178.

[7] Taylor CW, Kirby AM. Cardiac side-effects from breast cancer radiotherapy. Clin Oncol. 2015;27(11):621–629.

[8] Berg M, Lorenzen EL, Jensen I, et al. The potential benefits from respiratory gating for breast cancer patients regarding target coverage and dose to organs at risk when applying strict dose limits to the heart: results from the DBCG HYPO trial. Acta Oncol. 2018;57(1):113–119.

[9] Taylor CW, Wang Z, Macaulay E, et al. Exposure of the heart in breast cancer radiation therapy: a systematic review of heart doses published during 2003 to 2013. Radiat Oncol Biol. 2015; 93(4):845–853.

[10] Jacob S, Camilleri J, Derreumaux S, et al. Is mean heart dose a relevant surrogate parameter of left ventricle and coronary arteries exposure during breast cancer radiotherapy: a dosimetric evaluation based on individually-determined radiation dose (BACCARAT study). Radiat Oncol. 2019;14(1):29.

[11] Taylor C, McGale P, Brønnum D, et al. Cardiac structure injury after radiotherapy for breast cancer: cross-sectional study with individual patient data. J Clin Oncol. 2018;36(22):2288–2296.

[12] Stick LB, Lorenzen EL, Yates ES, et al. Selection criteria for early breast cancer patients in the DBCG proton trial - the randomised phase III trial strategy. Clin Transl Radiat Oncol. 2021;27:126–131.

[13] Finnegan R, Lorenzen EL, Dowling J, et al. Analysis of cardiac substructure dose in a large, multi-centre Danish breast cancer cohort (the DBCG HYPO trial): trends and predictive modelling. Radiother Oncol. 2020;153:130–138.

[14] Duane F, Aznar MC, Bartlett F, et al. A cardiac contouring atlas for radiotherapy. Radiother Oncol. 2017;122(3):416–422.

[15] Milo MLH, Offersen BV, Bechmann T, et al. Delineation of whole heart and substructures in thoracic radiation therapy: national guidelines and contouring atlas by the Danish multidisciplinary cancer groups. Radiother Oncol. 2020;150:121–127.

[16] van den Bogaard VAB, van Dijk LV, Vliegenthart R, et al. Development and evaluation of an auto-segmentation tool for the left anterior descending coronary artery of breast cancer patients based on anatomical landmarks. Radiother Oncol. 2019; 136:15–20.

[17] Levis M, De Luca V, Fiandra C, et al. Plan optimization for mediastinal radiotherapy: estimation of coronary arteries motion with ECG-gated cardiac imaging and creation of compensatory expansion margins. Radiother Oncol. 2018;127(3):481–486.

[18] Loap P, Tkatchenko N, Nicolas E, et al. Optimization and auto-segmentation of a high risk cardiac zone for heart sparing in breast cancer radiotherapy. Radiother Oncol. 2020;153:146–154.

[19] Kaderka R, Gillespie EF, Mundt RC, et al. Geometric and dosimetric evaluation of atlas based auto-segmentation of cardiac structures in breast cancer patients. Radiother Oncol. 2019;131: 215–220.

[20] Finnegan R, Dowling J, Koh ES, et al. Feasibility of multi-atlas cardiac segmentation from thoracic planning CT in a probabilistic framework. Phys Med Biol. 2019;64(8):085006.

[21] Maffei N, Fiorini L, Aluisio G, et al. Hierarchical clustering applied to automatic atlas based segmentation of 25 cardiac Sub-structures. Phys Med. 2020;69:70–80.

[22] Loap P, Tkatchenko N, Kirova Y. Evaluation of a delineation software for cardiac atlas-based autosegmentation: an example of the use of artificial intelligence in modern radiotherapy. Cancer Radiother. 2020;24(8):826–833.

[23] Morris ED, Ghanem AI, Pantelic MV, et al. Cardiac substructure segmentation and dosimetry using a novel hybrid magnetic resonance and computed tomography cardiac atlas. Int J Radiat Oncol Biol Phys. 2019;103(4):985–993.

[24] Jung JW, Lee C, Mosher EG, et al. Automatic segmentation of cardiac structures for breast cancer radiotherapy. Phys Imaging Radiat Oncol. 2019;12:44–48.

[25] Zhou R, Liao Z, Pan T, et al. Cardiac atlas development and validation for automatic segmentation of cardiac substructures. Radiother Oncol. 2017;122(1):66–71.

[26] John P, Nelson A, Harper J, et al. Deformable image registration in MIM maestroTM evaluation and description. MIM Softw Inc; 2013. p. 1–5.

[27] Warfield SK, Zou KH, Wells WM. Simultaneous truth and performance level estimation (STAPLE): an algorithm for the validation of image segmentation. IEEE Trans Med Imaging. 2004;23(7): 903–921.

[28] Albertson TE, Sutter ME, Chan AL. The acute management of asthma. Clin Rev Allergy Immunol. 2015;48(1):114–125.

[29] Shahoud JS, Ambalavanan M, Tivakaran VS. Cardiac Dominance; 2019. https://pubmed.ncbi.nlm.nih.gov/30725892/